

Research Article

Surface Enamel Remineralization: Biomimetic Apatite Nanocrystals and Fluoride Ions Different Effects

Norberto Roveri,¹ Elisa Battistella,² Claudia Letizia Bianchi,³ Ismaela Foltran,^{1,2} Elisabetta Foresti,¹ Michele Iafisco,^{1,2} Marco Lelli,¹ Alberto Naldoni,³ Barbara Palazzo,^{1,2} and Lia Rimondini²

¹ Department of Chemistry "G. Ciamician", University of Bologna, Via Selmi 2, 40126 Bologna, Italy

² Department of Medical Sciences, University of Eastern Piedmont "Amedeo Avogadro", Via Solaroli 17, 28100 Novara, Italy

³ Department of Physical Chemistry and Electrochemistry, University of Milano, Via Golgi 19, 20133 Milano, Italy

Correspondence should be addressed to Norberto Roveri, norberto.roveri@unibo.it

Received 13 October 2008; Accepted 22 January 2009

Recommended by Alan K. T. Lau

A new method for altered enamel surface remineralization has been proposed. To this aim carbonate-hydroxyapatite nanocrystals which mimic for composition, structure, nanodimensions, and morphology dentine apatite crystals and resemble closely natural apatite chemical-physical properties have been used. The results underline the differences induced by the use of fluoride ions and hydroxyapatite nanocrystals in contrasting the mechanical abrasions and acid attacks to which tooth enamel is exposed. Fluoride ions generate a surface modification of the natural enamel apatite crystals increasing their crystallinity degree and relative mechanical and acid resistance. On the other hand, the remineralization produced by carbonate-hydroxyapatite consists in a deposition of a new apatitic mineral into the eroded enamel surface scratches. A new biomimetic mineral coating, which progressively fills and shadows surface scratches, covers and safeguards the enamel structure by contrasting the acid and bacteria attacks.

Copyright © 2009 Norberto Roveri et al. This is an open access article distributed under the Creative Commons Attribution License, which permits unrestricted use, distribution, and reproduction in any medium, provided the original work is properly cited.

1. Introduction

Dental erosion is the chemical wear of the dental hard tissue without the involvement of bacteria [1]. Its clinical relevance is becoming wider and wider [2–6], and it is considered one of the main tooth pathologies able to cause patient discomfort, after periodontal diseases and caries.

Its aetiology is related to the enormous increase in consumption of soft drinks, fruit juices and sport drinks consumption [7]. However, other acid sources such as drugs containing syrups, analgesics and vitamin C intake and environmental acid exposure in working conditions are claimed to be related to enamel erosion [8–12].

The mechanisms involved in the damage of dental hard tissue are the acid attacks on the outer few micrometers of the enamel, which brings to demineralization and dissolution of the mineral phase [13–16].

Hydroxyapatite is the main constituent of the dental tissues representing in enamel and dentine the 95 wt% and 75 wt%, respectively.

The primary determinant of dissolution rate is the solubility of hydroxyapatite (HA) which is related to pH, and the presence of salivary pellicle also appears to be important [17–19].

Frequent application of a high concentration of topical fluoride may be of some benefit in preventing further demineralization and increasing the abrasion resistance of erosion lesions [20].

In vitro studies have shown that synthetic carbonated-hydroxyapatite (CHA) dissolution inhibition is a logarithmic function of the fluoride concentration in solution [21].

Systemic intake of fluoride during tooth formation has been claimed to be effective in caries prevention just by means of the apatite demineralization inhibition. According

to recommended daily allowances (RDAs) panel of the European Food Safety Authority, an intake of 0.1 mg fluoride/Kg body weight/day in children up to the age of eight years can be considered as the dose below which there will be no significant occurrence of moderate forms of fluorosis in permanent teeth [22].

However, it is important to consider that fluoridated water, fluoride supplements in diet, fluoride toothpaste, and topical fluoride applications have been identified as sources of enamel fluorosis [23]. Moreover, the “probably toxic dose” of fluoride—the dose which should trigger therapeutic intervention and hospitalization—is 5 mg/Kg of body weight, but as currently packaged, many dental products contain sufficient fluoride to exceed the “probably toxic dose” for young children [24].

Most of the products and devices used to contrast enamel and dentine erosion, such as fluoride [25–28], behave by reducing apatite dissolution rather than aiming to promote mineralization through apatite crystallization or replacement of the lost mineral. Hydroxyapatite, as well as in bone, is responsible for the mechanical behavior of the dental tissues. Unlike bone, in enamel and dentine, when HA is dissolved or abraded, it cannot spontaneously remineralize because enamel contains no cells and dentine apposition occurs only toward the pulp tissues. Therefore, both enamel and dentine can be reconstructed only by the application of alloplastic materials providing a sort of prosthetic restoration. In view of this situation, the demineralized area and micrometric sized scratches, which normally occur on enamel surface as a consequence of microwear and acid attack [29], cannot be repaired biologically nor prosthetically.

Hydroxyapatite has been widely subjected to experiment as bone filler and prosthetic coating due to its biocompatibility and osteoconductivity, representing an elective material covering a wide range of applications for bone substitution and interface [30]. Poorly crystalline HA nanocrystals, in addition to the excellent biological properties of HA, such as nontoxicity and lack of inflammatory and immunity responses, have bioresorption properties under physiological conditions. This property can be modulated by modifying its degree of crystallinity, which is achieved by implementation of innovative synthesis with a nanosize crystals control. In the last decade, advanced technology has been utilized to synthesize a new generation of biomimetic apatitic alloplastic materials which can optimize the interaction with biological entities thanks to their strong surface bioactivity [31]. The aim of the present study is to highlight the effect of the synthetic biomimetic hydroxyapatite crystals respect the fluoride ions into the remineralization in vitro of human enamel surface.

2. Materials and Methods

2.1. Chemicals. All the chemicals reagents used were of high chemical grade from Sigma-Aldrich, Mo, USA.

2.2. Synthesis of Carbonate-Hydroxyapatite Nanocrystals. Plate-acicular shaped carbonate-hydroxyapatite nanocrystals

about 100 nm in size were synthesized according to a modification of the method previously reported [32] and patented [33]. CHA nanocrystals about 100 nm in size were precipitated from an aqueous suspension of $\text{Ca}(\text{OH})_2$ (0.17 M) by slow addition of H_3PO_4 (0.15 M). The reaction mixture was stirred at 37°C for 12 hours, and then stirring was suspended allowing the deposition of CHA nanocrystals. Synthesized CHA 100 nm sized nanocrystals were isolated by filtration of the mother liquor, repeatedly washed with water and freeze-dried. The fraction of plate-acicular shaped crystals about 100 nm in size with a granular dimensions ranging from 100 to 150 μm was selected for the study. Aliquot of plate-acicular shaped crystals about 100 nm in size has been allowed, after synthesis to intergrowth in the reaction mixture up to the formation of clusters having dimension ranging from about 0.5 to 3.0 μm . The cluster aggregation process has been stopped by adding a surfactant (Protelan MST35 8 wt%) in the mother solution.

Plate-shaped carbonate-hydroxyapatite nanocrystals about 20 nm sized were synthesized according to the method of Liou et al. [34] with some modifications. The nanocrystals were precipitated from an aqueous solution of $(\text{NH}_4)_3\text{PO}_4$ (5.1 mM) by slow addition of an aqueous solution of $\text{Ca}(\text{CH}_3\text{COO})_2$ (8.5 mM) keeping the pH at a constant value of 10 by addition of a NH_4OH solution. The reaction mixture was kept under stirring at room temperature for 24 hours, and then stirring was suspended allowing the deposition CHA nanocrystals. Synthesized CHA nanocrystals were isolated by filtration of the solution, repeatedly washed with water, and freeze-dried. The fraction of plate shaped crystals about 20 nm in size having granular dimensions ranging from 100 to 150 μm was selected for the study.

2.3. Morphological Characterization. Transmission electron microscopy (TEM) investigations were carried out using a Philips CM 100 instrument. The powdered samples were ultrasonically dispersed in ultrapure water, and then a few droplets of the slurry deposited on holey-carbon foils supported on conventional copper microgrids.

Scanning electron microscopy (SEM) observation was carried out by an SEM (Zeiss EVO, 40 XVP) using secondary electrons at 25 kV and various magnifications.

2.4. Structural Characterization. X-ray diffraction powder and enamel surface patterns were collected using an Analytical X'Pert Pro equipped with X'Celerator detector powder diffractometer using $\text{Cu K}\alpha$ radiation generated at 40 kV and 40 mA. The instrument was configured with a 1° divergence and 0.2 mm receiving slits. The samples were prepared using the front loading of standard aluminium sample holders which are 1 mm deep, 20 mm high, and 15 mm wide. The degree of HA crystallinity was evaluated according to the formula [35]

$$\text{crystallinity} = \left(\frac{X}{Y} \right) 100, \quad (1)$$

where X = net area of diffracted peaks, and Y = net area of diffracted peaks + background area.

Crystal domain size along the c direction was calculated applying Scherrer's formula

$$L_{(002)} = \frac{0.94\lambda}{\left[\cos \theta \left(\sqrt{\Delta r^2 - \Delta_0^2} \right) \right]}, \quad (2)$$

where θ is the diffraction angle for plane (002), Δr and Δ_0 are the widths in radians of reflection (002) at half height for the synthesized and the reference HA materials, respectively, and $\lambda = 1.5405 \text{ \AA}$.

2.5. Infrared Microscopy Spectral Analysis. ATR-IR spectra were recorded on a Thermo Nicolet 380 FT-IR spectrometer equipped with a commercial ATR accessory.

The infrared spectra were registered from 4000 to 400 cm^{-1} at 2 cm^{-1} resolution using a Bruker IFS 66v/S spectrometer using KBr pellets.

ATR spectra were recorded with the cell empty to be used as a blank for subsequent experiments. Samples were made by placing the powder sample onto the Ge ATR crystal. Spectra were collected by averaging 32 scans at 4 cm^{-1} resolution.

2.6. Specific Surface Area Determination. Measurements were undertaken using a Carlo Erba Sorptly 1750 instrument by measuring N_2 absorption at 77 K and adopting the well-known BET procedure [36].

2.7. Spectrophotometric Analysis. Phosphorus contents were determined spectrophotometrically as molybdovanadophosphoric acid using 1 cm quartz cell [37].

Calcium contents were measured using inductively coupled plasma (ICP) optical emission spectrometry (OES) using a Perkin Elmer Optima 4200 DV.

2.8. X-Ray Photoemission Spectroscopy (XPS). Analyses were performed in an M-Probe Instrument (SSI) equipped with a monochromatic Al $K\alpha$ source (1486.6 eV) with a spot size of 200 \times 750 μm and pass energy of 25 eV, providing a resolution for 0.74 eV. With a monochromatic source, an electron flood gun was used to compensate the build up of positive charge on the insulator samples during the analyses. 10 eV electrons were selected to perform measurements on these samples. The accuracy of the reported binding energies (BEs) was estimated to be ± 0.2 eV. The quantitative data were also accurately checked and reproduced several times (at least ten times for each sample), and the percentage error was estimated to be $\pm 1\%$.

2.9. Statistics Analysis. Determination of HA crystallite domain size along the c direction, bulk and surface Ca/P ratio, and specific surface area were carried out 5 times on the same synthesis product. Data are presented as mean value \pm SD. Differences were considered statistically significant at a significance level of 90%.

2.10. In Vitro Enamel Remineralization Procedures. Slabs of enamel (3 \times 3 mm) were obtained from interproximal

surfaces of premolars extracted for orthodontic reasons. After the extraction, the teeth were cut with diamond disks, and the obtained slabs were sonicated for 10 minutes in 50% ethanol in order to remove any debris. Then, the specimens were etched with 37% phosphoric acid for 1 minute. Etched slabs were washed in distilled water for 10 minutes under stirring and then air dried. Two different in vitro remineralization procedures have been performed.

The first in vitro remineralization procedure utilizes a 10 wt% CHA in the range from 100 to 150 μm granules slurries constituted of both 20 nm or 100 nm sized nanocrystals. CHA nanocrystals aqueous slurries were applied for 10 minutes on the surfaces of the enamel slabs at room temperature with 100% relative humidity and then removed by water washing and air dried.

The second in vitro remineralization process utilizes toothpaste containing both fluoride ions and CHA 0.5–3.0 μm sized clusters constituted by intergrowth of 100 nm sized nanocrystals.

Comparable etched enamel slabs were divided into 3-groups of treatment using, respectively, fluoride or CHA-based toothpaste and only water (control). Each slab was brushed three times a day for a period of 15 days. The intervals between brushing sessions were at least 5 hours. Every brushing session has been performed for 30 seconds by an electric toothbrush using constant pressure and a bean sized toothpaste aliquot wetted with tap water, closely resembling the in vivo usual tooth brushing procedure. After every treatment, the single enamel slab was washed with tap water using a cleaned toothbrush in order to remove residual toothpaste.

3. Results

3.1. Synthesis and Characterization of Biomimetic Carbonate-Hydroxyapatite Nanocrystals. Biomimetic carbonate-hydroxyapatite nanocrystals have been synthesized with a nearly stoichiometric in bulk Ca/P molar ratio of about 1.6–1.7 and containing 4 ± 1 wt% of carbonate ions replacing prevalently phosphate groups. CHA nanocrystals have been synthesized both about 100 nm and 20 nm sized with an acicular and plate morphology, respectively. TEM images of synthetic 20 nm sized CHA nanocrystals showing the plate-shaped morphology and synthetic 100 nm sized CHA nanocrystals showing the acicular morphology are reported in Figures 1(a) and 1(b), respectively.

CHA nanocrystals can aggregate in microsized crystal clusters, whose dimensions increase prolonging maturation time in mother solution at constant temperature and stirring [33].

Powder X-ray diffraction patterns of plate shaped about 20 nm sized CHA nanocrystals and acicular shaped about 100 nm sized CHA nanocrystals (see Figures 2(b) and 2(c), resp.) show characteristic diffraction maxima of an apatite single phase (JCPDS 01-074-0565).

These X-ray diffraction patterns are compared with those collected for natural carbonate hydroxyapatite from deproteinized dentine and enamel reported in Figures 2(a)

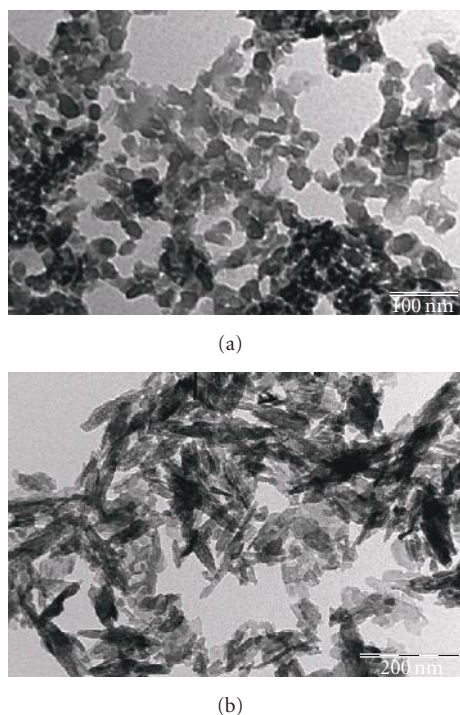


FIGURE 1: TEM images of (a) synthetic plate-shaped 20 nm sized CHA nanocrystals (scale bar = 100 nm), (b) synthetic plate-acicular 100 nm sized CHA nanocrystals (scale bars = 200 nm).

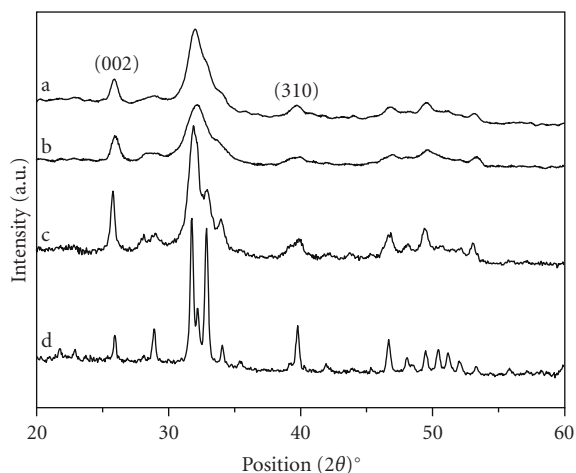


FIGURE 2: X-ray diffraction patterns of (a) natural carbonate-hydroxyapatite from deproteinized dentine, (b) synthetic plate shaped 20 nm sized CHA nanocrystals, (c) synthetic plate-acicular shaped 100 nm sized CHA nanocrystals, and (d) natural carbonate-hydroxyapatite from enamel.

and 2(d), respectively. The broadening of the diffraction maxima present in the X-ray diffraction patterns reported in Figures 2(a), 2(b), and 2(c) indicates a relatively low degree of crystallinity, which was quantified according to previous [35]. The degree of crystallinity of synthesized about 20 nm sized CHA nanocrystals with plate morphology and synthesized about 100 nm sized CHA nanocrystals with acicular

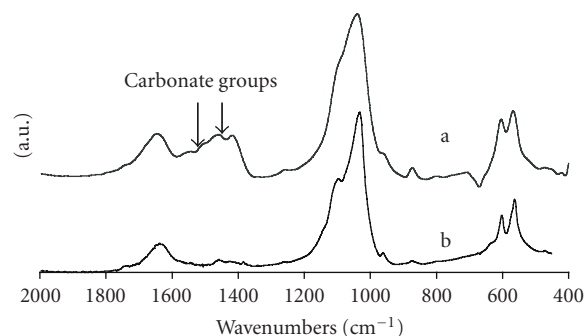


FIGURE 3: (a) FTIR spectra of synthetic 20 nm sized CHA nanocrystals, (b) natural carbonate-hydroxyapatite from deproteinized dentine.

morphology is 30% and 50%, respectively. The crystallinity degree of about 20 nm sized CHA nanocrystals is very close to that one determined from the X-ray diffraction pattern of deproteinized dentine natural carbonate-hydroxyapatite (28%) reported in Figure 2(a). Furthermore, the crystallinity degree of natural hydroxyapatite of deproteinized enamel, reported in Figure 2(d), is 70%. The crystal domain sizes along the c direction have been calculated by Scherrer's formula using the $2\theta = 26^\circ$ (002) diffraction peak of the X-ray diffraction patterns reported in Figures 2(a), 2(b), and 2(c). The calculated crystal domain sizes for 20 nm sized CHA nanocrystals and deproteinized dentine are 250 Å and 213 Å, respectively. These results obtained by X-ray diffraction investigation reveal that the crystal structures of the synthesized CHA nanocrystals are very close to that observed for natural dentine.

The same similarity can be observed from the comparison of the FTIR spectra of synthesized CHA nanocrystals and natural apatite of deproteinized dentine reported in Figures 3(a) and 3(b), respectively. In these spectra, the characteristic absorption bands of phosphate and carbonate groups are clearly resolved. The absorption band at 1468 cm^{-1} is related to the carbonate group substitution to the phosphate one, while the shoulder at 1545 cm^{-1} can be considered the contribution of the carbonate group substituting the hydroxyl group in the apatite structure. This finding reveals that synthesized CHA nanocrystals not only contain a similar carbonate amount, but also underline that the carbonate substitution to the phosphate and/or hydroxyl group is very similar in the synthetic and biological crystals.

A surface characterization of the synthetic carbonate-hydroxyapatite nanocrystals has been carried out in order to highlight their surface chemical-physical characteristic which directly interfaces and reacts with exposed dental tissues. The ATR spectra (data not shown) of the synthetic about 20 nm and 100 nm sized CHA nanocrystals reveal a 4% and 3 wt% surface carbonate, respectively. The consistent amount of surface of carbonate percentage present in synthetic CHA is appreciably higher than the surface carbonate percentage present in enamel and dentine about 2 wt%.

Specific surface area of $100 \text{ m}^2 \text{ g}^{-1}$ and $80 \text{ m}^2 \text{ g}^{-1}$ has been determined for 20 nm sized CHA nanocrystals with plate

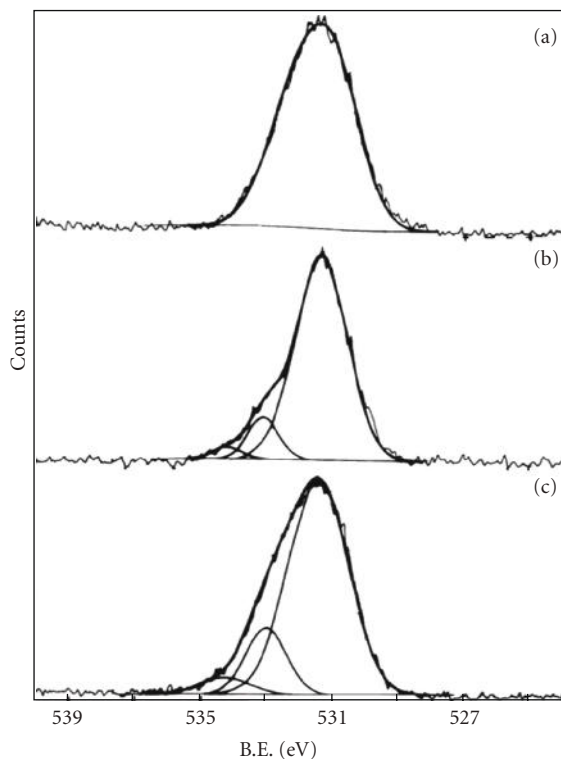
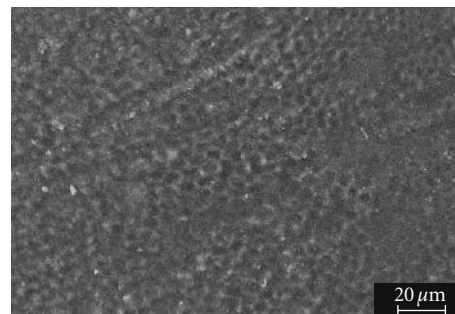


FIGURE 4: XPS analysis of spectral features of (a) the O 1s region of the enamel demineralized by orthophosphoric acid 37% for 1 minute, (b) enamel remineralized by a treatment with synthetic microclusters of CHA nanocrystals 100 nm sized for 10 minutes, and (c) synthetic microclusters of CHA nanocrystals 100 nm sized.

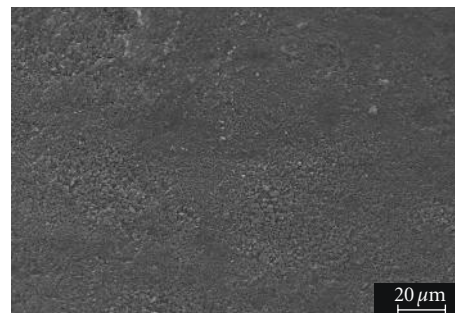
morphology and synthesized 100 nm sized CHA nanocrystals with acicular morphology, respectively. These specific surface area values obtained for synthetic nanocrystals are only slightly lower than the $110 \text{ m}^2\text{g}^{-1}$ obtained for biological nanocrystals.

The surface Ca/P molar ratio determined by XPS analysis for CHA nanocrystals and CHA crystals microclusters does not reveal appreciable differences and result significantly lower than Ca/P molar ratio determined by ICP analysis in bulk indicating a surface calcium deficiency probably due to surface disorder. In fact, the Ca/P molar ratios of 1.7 determined in bulk for synthetic CHA nanocrystals reduce to a value of 1.4-1.5 when determined on the crystals surface by XPS analysis (see Table 1). XPS analysis of spectral features of the O 1s region of the synthetic 100 nm sized CHA nanocrystals (see Figure 4(c)) shows a definite O 1s shape fitted by three components: a first, very intense, peak at lower BE attributed to oxygen in phosphate group, a second peak due to OH of the carbonate-hydroxyapatite, and a final peak at very high BE, which can be attributed to trapped undissociated water and carbonates.

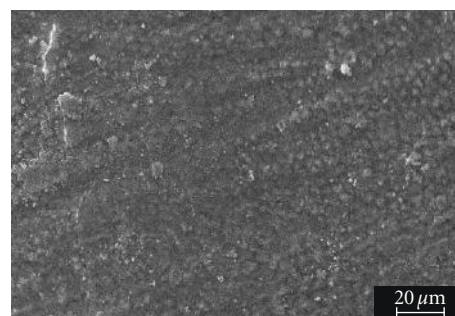
3.2. In Vitro Enamel Surface Remineralization by Biomimetic CHA Nanocrystals. SEM analysis allows investigating the morphology of both demineralized enamel and the fea-



(a)



(b)



(c)

FIGURE 5: SEM image of enamel surface after application of 37% orthophosphoric acid for 1 minutes. The etching treatment removed aprismatic layer and exposed prismatic and interprismatic hydroxyapatite structures (a), remineralized enamel surface after treatment by synthetic CHA micro-clusters constituted of nanocrystals 20 nm (b) and 100 nm sized (c) and synthetic CHA micro-clusters.

tures observed after remineralization procedures induced by biomimetic CHA nanocrystals in vitro application.

The demineralization procedure by orthophosphoric acid 37% for 1 minute removes the aprismatic enamel, and exposed hydroxyapatite prisms became evident. Figure 5(a) shows demineralization of both interprismatic and prismatic enamel structures.

After treatment for 10 minutes by aqueous slurry of both synthetic 20 nm and 100 nm sized CHA nanocrystals, the surface of the demineralized enamel appears covered by the CHA phase (see Figures 5(b) and 5(c), resp.) arranged in a thick and homogeneous apatitic layer.

XPS analysis of spectral features of the O 1s region of the enamel demineralized by orthophosphoric acid 37%

TABLE 1: XPS analysis of CHA nanocrystals, enamel tooth treated with ortophosphoric acid before and after treatment with either CHA 20 or 100 nm sized nanocrystals and after brushing with toothpaste containing booth CHA or fluoride.

Sample	O (%)	C (%)	Ca (%)	P (%)	N (%)	Si (%)	Na (%)	F (%)	Ca/P
20 nm CHA nanocrystals	50.4	17.6	19.4	12.6	—	—	—	—	1.5
100 nm CHA nanocrystals	48.4	18.0	19.6	13.9	—	—	—	—	1.4
Tooth treated with ortophosphoric acid	30.7	49.4	5.4	5.3	5.9	1.9	1.4	—	1.1
Tooth treated with 20 nm CHA nanocrystals	43.3	27.3	13.4	10.1	2.3	—	1.9	—	1.3
Tooth treated with 100 nm CHA nanocrystals	43.7	26.0	14.8	11.2	1.0	—	1.5	—	1.3
CHA containing toothpaste	30.7	51.9	5.5	4.7	1.6	5.6	—	—	1.2
Fluoride containing toothpaste	20.9	63.3	4.1	1.2	2.0	4.9	—	3.6	3.4

for 1 minute shows a single broad band, in which it is difficult to determine precisely and to quantify the binding energy (BE) and, therefore, the kind of the surface oxygen components (see Figure 4(a)). On the contrary, the enamel remineralized by synthetic 100 nm sized CHA nanocrystals for 10 minutes shows a definite O 1s shape fitted by three components at different binding energy (see Figure 4(b)). These components correspond to the same three ones used to fit O 1s shape recorded for synthetic 100 nm sized CHA nanocrystals (see Figure 4(c)), the first at lower BE very intense peak is attributed to oxygen in phosphate group, the second peak is due to OH of the carbonate-hydroxyapatite, and a final peak at high BE, can be attributed to trapped undissociated water and carbonate groups. These results unequivocally confirm the presence of synthetic CHA at the surface of the treated enamel and the consequent validation of the enamel remineralization. The same finding is pointed out by the ATR spectrum of enamel treated for 10 minutes by synthetic 100 nm sized CHA nanocrystals, showing appreciable higher intensity of the characteristic absorption bands of carbonate ions (1420–1460 and 1680 cm^{-1}) in respect of the same absorption bands present in the demineralized enamel ATR spectrum. No differences are appreciable in the phosphate ions bands (1000–1100 and 530–580 cm^{-1}). ATR spectrum (data not shown) of remineralized enamel reveals that surface apatite is richer in carbonate than natural one, such as synthetic 100 nm sized CHA nanocrystals.

3.3. In Vitro Enamel Surface Remineralization by Toothpaste Containing either Fluoride or Biomimetic CHA Nanocrystals Microclusters. SEM analysis allowed us to investigate the morphology of both demineralized enamel and the features observed after a remineralization process which utilizes in vitro application of toothpaste containing either fluoride or CHA microclusters constituted of 100 nm in size nanocrystals.

The surfaces of the teeth treated with fluoride (see Figure 6(b)) were not consistently changed respect to that of demineralization by ortophosphoric acid (see Figure 6(c)). Actually both the interprismatic and prismatic enamel structures appear still evident. On the contrary after treatment of the enamel slabs with a toothpaste containing synthesized CHA microclusters constituted of 100 nm sized nanocrystals, the interprismatic and prismatic enamel structures appear to

be completely hidden by a thick homogeneous apatitic layer (see Figure 6(a)).

The XRD patterns collected on the surface of enamel slabs after treatment with CHA or fluoride toothpaste and water are reported in Figures 7(b), 7(c), and 7(d), respectively, and compared with the XRD pattern (see Figure 7(a)) of CHA microclusters constituted of 100 nm sized nanocrystals utilized to prepare the used CHA toothpaste. The XRD diffraction maxima recorded on the surface of enamel slabs treated with fluoride containing toothpaste appear slightly more sharpened than those obtained on the enamel etched slabs brushed only with water. This observation reveals an increased crystallinity degree probably due to a partial structural conversion of hydroxyapatite into fluoride substituted hydroxyapatite. On the contrary, the XRD pattern obtained on the surface of enamel slabs brushed with CHA containing toothpaste shows the broadened diffraction maxima characteristic of the synthetic biomimetic CHA, revealing its presence on the enamel surface. The CHA not removed by brushing procedures suggests the formation of chemical bonds between the synthetic CHA microclusters constituted of 100 nm sized nanocrystals and natural enamel apatite crystals. These bonds allow the formation of a persistent CHA coating on the enamel surface whose morphology was detected by SEM analysis.

The surface Ca/P molar ratio determined by XPS analysis for demineralized enamel slabs before and after in vitro remineralization by brushing whit toothpaste containing either fluoride or CHA are compared in Table 1. In this table, a comparison with the Ca/P molar ratio of CHA microclusters constituted of 100 nm sized nanocrystals also present. The enamel surface Ca/P molar ratio changes before and after the brushing treatment with toothpaste containing fluoride, assuming a value of 3.4 very different from the apatite stoichiometric one (Ca/P = 1.7). This finding reveals that the only structural modification of enamel hydroxyapatite induced by fluoride is restricted to a partial hydroxyl groups replacement by fluoride ions without affecting appreciably the Ca and phosphate structural network. On the contrary, enamel slabs treated with the toothpaste containing synthesised CHA microclusters of 100 nm sized nanocrystals exhibit a surface Ca/P molar ratio very similar to that one of the synthetic CHA.

This coating is highly less crystalline than native enamel apatite, and consists of a new apatitic mineral deposition

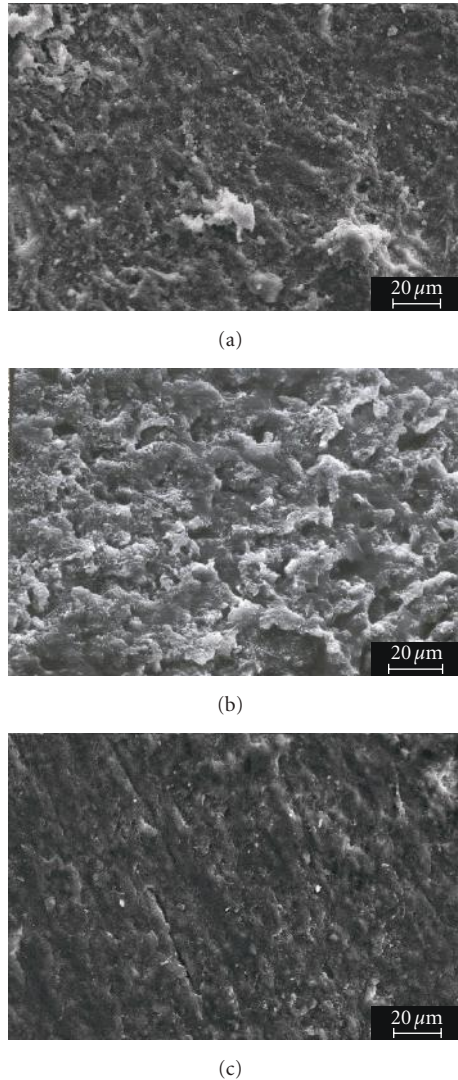


FIGURE 6: SEM images of enamel after brushing treatment with (a) CHA toothpaste containing, (b) fluoride containing toothpaste, and (c) orthophosphoric acid application.

which progressively fills the scratches and pits. On the contrary, the surface remineralization observed on the specimens treated with fluoride containing toothpaste is mainly based on chemical-physical enamel apatite surface modifications rather than a formation of a new mineral deposition.

The CHA biomimetic coating formation is a remineralization process corresponding to a new apatite deposition in the demineralized area of enamel surface.

4. Discussion

Enamel is the hardest and most mineralized tissue of human body. It is structured in order to resist to mechanical injuries, abrasion, and chemical attack. Differently from all the other mineralized tissues, it lacks proteins even if they are essential to its formation. Actually, matrix proteins are

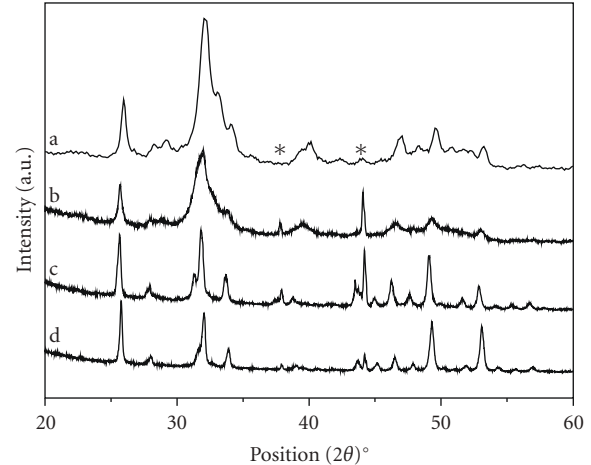


FIGURE 7: (a) XRD pattern of synthetic CHA, (b) enamel after brushing treatment with CHA containing toothpaste, (c) enamel after brushing treatment with fluoride containing toothpaste, (d) enamel after brushing treatment with water. *indicates Al holder diffraction maxima.

cleaved by proteinases secreted by the ameloblasts during tooth formation; hence, the matrix proteins of enamel are not incorporated into enamel prisms [38]. Degradation and resumption of enamel matrix proteins is the reason why enamel prisms, once formed, cannot be remodelled. After enamel prism formation, only the amount of hydroxyapatite within the prisms may decrease in consequence of chemical changes into the oral environment.

Acid attack is one of the major causes of enamel hydroxyapatite loss. It may occur even in young age as a consequence of plaque metabolism or simply due to food and beverage intakes [2–4].

In the present paper, synthetic carbonate-hydroxyapatite biomimetic nanocrystals have been chemical-physical characterized and investigated regarding the possibility to obtain an *in vitro* remineralization of the altered enamel surfaces.

The experimental model used in the present investigation was the demineralization by means of orthophosphoric acid of sound enamel of the interproximal surfaces and its subsequent remineralization.

This model was chosen because the demineralizing effect of orthophosphoric acid is well known in terms of chemical and microhistological features because it is an essential part of the procedures of adhesive restoration applications.

The SEM observations showed that the enamel is characterized by both amorphous and prismatic hydroxyapatite and by an irregular surface even. The use of orthophosphoric acid causes an exposure of prism and a loss of both interprismatic and prismatic substances.

The treatment of demineralized enamel only for ten minutes, by synthetic CHA nanocrystals, induces a consistent enamel remineralization through the formation of a surface carbonate-hydroxyapatite coating. This coating is due to the chemical bond of the synthetic CHA nanocrystals biomimetic for composition, structure, size, and morphology on the surface prismatic hydroxyapatite enamel. It can

be supposed that the application of CHA nanocrystals 20 nm sized allows a better mineralization in the lower surface fissure, because the interprismatic and prismatic enamel structures appear totally hidden. Using an equal time of treatment, the application of CHA nanocrystals 100 nm sized produces the formation of a homogeneous coating which hides interprismatic and prismatic enamel structures when examined with SEM.

In this paper, an in vitro enamel surface remineralization by brushing with toothpaste containing either fluoride or biomimetic CHA nanocrystals microclusters has been also carried out. The XRD patterns, SEM images, and XPS spectra collected on the surface of enamel slabs before and after treatment with CHA or fluoride toothpaste underline the possibility to obtain an enamel remineralization through the formation of a surface apatite coating which covers the enamel structure avoiding the most probably health dangerous fluoride effects, to contrast the mechanical abrasion and acid attacks to which tooth enamel is exposed. The documented CHA biomimetic coating formation which is less crystalline than enamel natural apatite represents an enamel repair process corresponding to an apatite deposition inside the demineralized area of enamel surface and may be considered an innovative approach to contrast enamel demineralization.

Acknowledgments

The authors acknowledge financial support from the University of Bologna, C.I.R.C.M.S.B., the Italian Ministero dell'Istruzione, Università e Ricerca (MIUR) PRIN Project no. 2006-032335, and the COSWELL President Paolo Gualandi for his cheering eagerness in suggesting this research work.

References

- [1] J. D. Eccles, "Dental erosion of nonindustrial origin. A clinical survey and classification," *The Journal of Prosthetic Dentistry*, vol. 42, no. 6, pp. 649–653, 1979.
- [2] C. Deery, M. L. Wagner, C. Longbottom, R. Simon, and Z. J. Nugent, "The prevalence of dental erosion in a United States and a United Kingdom sample of adolescents," *Pediatric Dentistry*, vol. 22, no. 6, pp. 505–510, 2000.
- [3] C. R. Dugmore and W. P. Rock, "The prevalence of tooth erosion in 12-year-old children," *British Dental Journal*, vol. 196, no. 5, pp. 279–282, 2004.
- [4] Y. H. Al-Dlaigan, L. Shaw, and A. Smith, "Dental erosion in a group of British 14-year-old, school children—part I: prevalence and influence of differing socioeconomic backgrounds," *British Dental Journal*, vol. 190, no. 3, pp. 145–149, 2001.
- [5] I. B. Arnadóttir, S. R. Sæmundsson, and W. P. Holbrook, "Dental erosion in Icelandic teenagers in relation to dietary and lifestyle factors," *Acta Odontologica Scandinavica*, vol. 61, no. 1, pp. 25–28, 2003.
- [6] J. H. Nunn, P. H. Gordon, A. J. Morris, C. M. Pine, and A. Walker, "Dental erosion—changing prevalence? A review of British national childrens' surveys," *International Journal of Paediatric Dentistry*, vol. 13, no. 2, pp. 98–105, 2003.
- [7] British Soft Drinks Association, "A shared responsibility," Annual Report, The British Soft Drinks Association, London, UK, 2002–2003.
- [8] C. C. Costa, I. C. S. Almeida, and L. C. Costa Filho, "Erosive effect of an antihistamine-containing syrup on primary enamel and its reduction by fluoride dentifrice," *International Journal of Paediatric Dentistry*, vol. 16, no. 3, pp. 174–180, 2006.
- [9] M. Kitchens and B. M. Owens, "Effect of carbonated beverages, coffee, sports and high energy drinks, and bottled water on the in vitro erosion characteristics of dental enamel," *Journal of Clinical Pediatric Dentistry*, vol. 31, no. 3, pp. 153–159, 2007.
- [10] A. Wiegand and T. Attin, "Occupational dental erosion from exposure to acids—a review," *Occupational Medicine*, vol. 57, no. 3, pp. 169–176, 2007.
- [11] A. Lussi, T. Jaeggi, and D. Zero, "The role of diet in the aetiology of dental erosion," *Caries Research*, vol. 38, supplement 1, pp. 34–44, 2004.
- [12] A. Lussi, E. Hellwig, D. Zero, and T. Jaeggi, "Erosive tooth wear: diagnosis, risk factors and prevention," *American Journal of Dentistry*, vol. 19, no. 6, pp. 319–325, 2006.
- [13] N. X. West, A. Maxwell, J. A. Hughes, D. M. Parker, R. G. Newcombe, and M. Addy, "A method to measure clinical erosion: the effect of orange juice consumption on erosion of enamel," *Journal of Dentistry*, vol. 26, no. 4, pp. 329–335, 1998.
- [14] N. X. West, J. A. Hughes, D. M. Parker, R. G. Newcombe, and M. Addy, "Development and evaluation of a low erosive blackcurrant juice drink 2. Comparison with a conventional blackcurrant juice drink and orange juice," *Journal of Dentistry*, vol. 27, no. 5, pp. 341–344, 1999.
- [15] J. A. Hughes, N. X. West, D. M. Parker, R. G. Newcombe, and M. Addy, "Development and evaluation of a low erosive blackcurrant juice drink in vitro and in situ 1. Comparison with orange juice," *Journal of Dentistry*, vol. 27, no. 4, pp. 285–289, 1999.
- [16] J. A. Hughes, N. X. West, D. M. Parker, R. G. Newcombe, and M. Addy, "Development and evaluation of a low erosive blackcurrant juice drink 3. Final drink and concentrate, formulae comparisons in situ and overview of the concept," *Journal of Dentistry*, vol. 27, no. 5, pp. 345–350, 1999.
- [17] A. V. Nieuw Amerongen, C. H. Oderkerk, and A. A. Driessen, "Role of mucins from human whole saliva in the protection of tooth enamel against demineralization in vitro," *Caries Research*, vol. 21, no. 4, pp. 297–309, 1987.
- [18] B. T. Amaechi, S. M. Higham, W. M. Edgar, and A. Milosevic, "Thickness of acquired salivary pellicle as a determinant of the sites of dental erosion," *Journal of Dental Research*, vol. 78, no. 12, pp. 1821–1828, 1999.
- [19] Y. Nekrashevych and L. Stösser, "Protective influence of experimentally formed salivary pellicle on enamel erosion: an in vitro study," *Caries Research*, vol. 37, no. 3, pp. 225–231, 2003.
- [20] D. T. Zero and A. Lussi, "Erosion—chemical and biological factors of importance to the dental practitioner," *International Dental Journal*, vol. 55, no. 4, supplement 1, pp. 285–290, 2005.
- [21] J. D. B. Featherstone, R. Glana, M. Shariati, and C. P. Shields, "Dependence of in vitro demineralization of apatite and remineralization of dental enamel on fluoride concentration," *Journal of Dental Research*, vol. 69, pp. 620–625, 1990.
- [22] European Food Safety Authority, "Opinion of the scientific panel on dietetic products, nutrition and allergies on a request

- from the Commission related to the tolerable upper intake level of fluoride," *The EFSA Journal*, vol. 192, pp. 1–65, 2005.
- [23] D. G. Pendrys and J. W. Stamm, "Relationship of total fluoride intake to beneficial effects and enamel fluorosis," *Journal of Dental Research*, vol. 69, pp. 529–538, 1990.
- [24] G. M. Whitford, "The physiological and toxicological characteristics of fluoride," *Journal of Dental Research*, vol. 69, pp. 539–549, 1990.
- [25] C. Ganss, J. Klimek, U. Schäffer, and T. Spall, "Effectiveness of two fluoridation measures on erosion progression in human enamel and dentine in vitro," *Caries Research*, vol. 35, no. 5, pp. 325–330, 2001.
- [26] C. Ganss, J. Klimek, V. Brune, and A. Schürmann, "Effects of two fluoridation measures on erosion progression in human enamel and dentine in situ," *Caries Research*, vol. 38, no. 6, pp. 561–566, 2004.
- [27] A. Wiegand and T. Attin, "Influence of fluoride on the prevention of erosive lesions—a review," *Oral Health & Preventive Dentistry*, vol. 1, no. 4, pp. 245–253, 2003.
- [28] A. Young, P. S. Thrane, E. Saxegaard, G. Jonski, and G. Rölla, "Effect of stannous fluoride toothpaste on erosion-like lesions: an in vivo study," *European Journal of Oral Sciences*, vol. 114, no. 3, pp. 180–183, 2006.
- [29] M. F. Teaford, "A review of dental microwear and diet in modern mammals," *Scanning Microscopy*, vol. 2, no. 2, pp. 1149–1166, 1988.
- [30] N. Roveri and B. Palazzo, "Hydroxyapatite nanocrystals as bone tissue substitute," in *Tissue, Cell and Organ Engineering*, C. S. S. R. Kumar, Ed., vol. 9 of *Nanotechnologies for the Life Sciences*, pp. 283–307, Wiley-VCH, Weinheim, Germany, 2006.
- [31] B. Palazzo, M. Iafisco, M. Laforgia, et al., "Biomimetic hydroxyapatite-drug nanocrystals as potential bone substitutes with antitumor drug delivery properties," *Advanced Functional Materials*, vol. 17, no. 13, pp. 2180–2188, 2007.
- [32] E. Landi, A. Tampieri, G. Celotti, and S. Sprio, "Densification behaviour and mechanisms of synthetic hydroxyapatites," *Journal of the European Ceramic Society*, vol. 20, no. 14–15, pp. 2377–2387, 2000.
- [33] S. P. A. Coswell, G. Gazzaniga, N. Roveri, et al., "Biologically active nanoparticles of a carbonate-substituted hydroxyapatite, process for their preparation and compositions incorporating the same," EU patent no. 005146, 2006.
- [34] S.-C. Liou, S.-Y. Chen, H.-Y. Lee, and J.-S. Bow, "Structural characterization of nano-sized calcium deficient apatite powders," *Biomaterials*, vol. 25, no. 2, pp. 189–196, 2004.
- [35] Z. E. Erkmén, "The effect of heat treatment on the morphology of D-Gun sprayed hydroxyapatite coatings," *Journal of Biomedical Materials Research Part B*, vol. 48, no. 6, pp. 861–868, 1999.
- [36] S. Brunauer, P. H. Emmett, and E. Teller, "Adsorption of gases in multimolecular layers," *Journal of the American Chemical Society*, vol. 60, no. 2, pp. 309–319, 1938.
- [37] K. P. Quinlan and M. A. DeSesa, "Spectrophotometric determination of phosphorus as molybdovanadophosphoric acid," *Analytical Chemistry*, vol. 27, no. 10, pp. 1626–1629, 1955.
- [38] J. P. Simmer and A. G. Fincham, "Molecular mechanisms of dental enamel formation," *Critical Reviews in Oral Biology and Medicine*, vol. 6, no. 2, pp. 84–108, 1995.